The Iroquois Homeobox Gene 5 Is Regulated by 1,25-Dihydroxyvitamin D_3 in Human Prostate Cancer and Regulates Apoptosis and the Cell Cycle in LNCaP Prostate Cancer Cells

Anne Myrthue, Brooks L.S. Rademacher, Janet Pittsenbarger, Bozena Kutyba-Brooks, Marin Gantner, David Z. Qian, and Tomasz M. Beer

Abstract 1,25-Dihydroxyvitamin D_3 [$1,25(OH)_2D_3$], the most active metabolite of vitamin D_3, has significant antitumor activity in a broad range of preclinical models of cancer. In this study, we show that the Iroquois homeobox gene 5 (*Irx5*) is down-regulated by $1,25(OH)_2D_3$ in human prostate cancer samples from patients randomly assigned to receive weekly high-dose $1,25(OH)_2D_3$ or placebo before radical prostatectomy. Down-regulation of *Irx5* by $1,25(OH)_2D_3$ was also shown in the human androgen-sensitive prostate cancer cell line LNCaP and in estrogen-sensitive MCF-7 breast cancer cells. Knockdown of *Irx5* by RNA interference showed a significant reduction in LNCaP cell viability, which was accompanied by an increase in p21 protein expression, G_2-M arrest, and an increase in apoptosis. The induced apoptosis was partially mediated by p53, and p53 protein expression was increased as a result of *Irx5* knockdown. Cell survival was similarly reduced by *Irx5* knockdown in the colon cancer cell line HCT 116 and in MCF-7 breast cancer cells, each being derived from clinical tumor types that seem to be inhibited by $1,25(OH)_2D_3$. Overexpression of *Irx5* led to a reduction of p21 and p53 expression. This is the first report that *Irx5* is regulated by $1,25(OH)_2D_3$ in humans and the first report to show that *Irx5* is involved in the regulation of both the cell cycle and apoptosis in human prostate cancer cells. *Irx5* may be a promising new therapeutic target in cancer treatment.

1,25-Dihydroxyvitamin D_3 ($1,25(OH)_2D_3$) promises to be effective in the treatment and prevention of cancer. Numerous *in vitro* and *in vivo* studies have shown the ability of biologically active analogues of vitamin D to potently inhibit the proliferation of many different cell types, including carcinomas of the prostate, breast, colon, skin, brain, and myeloid leukemia cells (1, 2). $1,25(OH)_2D_3$ has also been shown to induce apoptosis in several tumor models (3–8) and to inhibit angiogenesis and tumor invasion (9–14). However, the molecular factors that mediate these processes have yet to be clearly defined.

Members of the Iroquois gene family play multiple roles in patterning and regionalization of embryonic tissues during development and are highly conserved from *Drosophila* to mammals (15–21). The Iroquois homeobox (*Irx*) genes were first identified in *Drosophila* because of their role in the control of proneural gene expression (16, 22). In *Drosophila*, the Iroquois gene cluster consists of three *Irx* genes, whereas in mammals, six genes exist in two clusters. The mammalian IrxA cluster (*Irx1*, *Irx5*, and *Irx4*) is located on chromosome 8, whereas the IrxB cluster (*Irx3*, *Irx2*, and *Irx6*) is found on chromosome 16. Iroquois protein products bind DNA, at least in part through their homeodomain motif, a highly conserved 63–amino acid sequence, and seem to act as both transcriptional activators and repressors (23–25). Outside the homeodomain, *Irx* family members share little sequence similarity, but all *Irx* transcription factors have a conserved motif called the Iro box.

Homeobox genes are developmental regulators that are essential for growth and differentiation, including early embryonic patterning, cell-type specification, and organogenesis. Increasing evidence indicate that normal development and tumorigenesis are intimately related, and the anomalous expression of many homeobox genes has been detected in a number of cancers, including prostate (26–29). Evidence that homeobox genes are involved in the regulation of proliferation through their interaction with several cell cycle regulators, including p21, p27, and cyclin D1, is accumulating (30). Recent data also suggest that homeobox genes play a role in regulating apoptosis, angiogenesis, and/or metastasis; however, very little is known about the specific signaling pathways involved (31, 32). A number of homeobox genes have been shown to be regulated by vitamin D (33).

Authors' Affiliation: Division of Hematology and Medical Oncology and OHSU Cancer Institute, Oregon Health and Science University, Portland, Oregon
Received 10/16/07; revised 1/10/08; accepted 2/12/08.
Grant support: William B. and Karen L. Early, Kenneth Jonsson Family Foundation, Oregon Health and Science University BioScience Innovation Fund, Department of Defense grant W81XWH-04-1-0832, and National Cancer Institute grant 1R21CA113380-01.
The costs of publication of this article were defrayed in part by the payment of page charges. This article must therefore be hereby marked *advertisement* in accordance with 18 U.S.C. Section 1734 solely to indicate this fact.
Requests for reprints: Tomasz M. Beer, Division of Hematology and Medical Oncology, Oregon Health and Science University, CH-14R, 3303 SW Bond Avenue, Portland, OR 97239. Phone: 503-494-0365; Fax: 503-494-6197; E-mail: beert@ohsu.edu.

doi:10.1158/1078-0432.CCR-07-4649

Materials and Methods

Chemicals. $1,25(OH)_2D_3$ was a kind gift from Dr. Milan Uskokovic, Hoffmann-La Roche. A 50^{-3} mol/L stock solution dissolved in absolute ethanol was stored at -80°C and protected from light.

Patients. The eligibility criteria and procedures of our randomized trial of high-dose $1,25(OH)_2D_3$ or placebo before prostatectomy have been previously described (34). Briefly, 44 patients were randomly assigned to receive $1,25(OH)_2D_3$ (0.5 μg/kg) or identical placebo weekly for 4 wk before prostatectomy. Prostatectomy was carried out 4 ± 1 d after the last dose of $1,25(OH)_2D_3$. Whereas the primary goal of the study was the interrogation of prostate cancer tissue for a series of biomarkers using immunohistochemistry in fixed specimens, snap-frozen tumor samples were obtained from a subset of patients for the purpose of exploratory studies of the effect of high-dose $1,25(OH)_2D_3$ on gene expression at the RNA level. After surgical removal, prostate tissues were embedded in Cryomatrix (Thermo Shandon), snap frozen in a solution of liquid pentane and dry ice, and stored at -80°C.

Cell lines. LNCaP and MCF-7 cells were obtained from American Tissue Culture Collection. Cells were subcultured every 48 to 72 h in RPMI 1640 (Invitrogen) supplemented with 10% fetal bovine serum (Invitrogen) and 1% penicillin/streptomycin (Invitrogen). Cells were incubated at 37°C with standard 5% CO_2 content in a humidified incubator. HCT 116 cells were a kind gift from Dr. Bert Vogelstein (Johns Hopkins University). HCT 116 cells were cultured in McCoy's 5A medium (Invitrogen) with 10% fetal bovine serum. The LNCaP p53 dominant-negative pC53Trp248 cells (248 mutant) and the control pRC-CMV were generously provided by Dr. Mark Garzotto (Portland VA Medical Center). The pC53Trp248 plasmid contains a mutant form of p53, which has a Trp substitution at the 248 position that allows it to inactivate wild-type p53. LNCaP cells stably transfected with the pC53Trp248 plasmid (LNCaP/p53DN) markedly overexpress dominant-negative p53 by immunoblot analysis compared with control (pRC-CMV)–transfected cells. Results from a transient transfection of LNCaP/p53DN cells with a p21 promoter-luciferase reporter plasmid showed that overexpression of the 248-p53 mutant inactivates the function of wild-type p53 in LNCaP cells (data not shown).

RNA extraction from human tumors. Snap-frozen human prostatectomy specimens containing ≥90% cancer (determined by histology analysis by a clinical pathologist) were pulverized by mortar and pestle in liquid nitrogen and homogenized in TRIzol reagent with a Tissue Tearor Homogenizer. RNA was extracted from the homogenized tissues according to the manufacturer's instructions (Life Technologies, Bethesda Research Laboratories).

Oligonucleotide microarrays. Labeled cRNA was prepared from 10 RNA samples: five individual cases [$1,25(OH)_2D_3$ treatment] and five individual placebo controls. Each sample target was hybridized to an HG-U133A Human GeneChip array (22,283 transcripts; Affymetrix). All quality control tests indicated good sample performance. Gene expression profiling was done in the Affymetrix Microarray Core of the Gene Microarray Shared Resource at Oregon Health and Science University.

RNA extraction from cell lines. LNCaP cells grown in 60-mm plates were washed with PBS and subsequently lysed in RSB lysis buffer [10 mmol/L Tris-HCl (pH 7.4), 150 mmol/L NaCl, 1.5 mmol/L MgCl, 0.65% NP40]. The lysate was centrifuged ($2,500 \times g$) at 4°C for 10 min, and RNA was extracted in 0.8 mL phenol and 0.4 mL urea buffer [7 mol/L urea, 350 mmol/L NaCl, 10 mmol/L Tris (pH 7.4), 100 mmol/L EDTA (pH 8.0), 1% SDS]. The aqueous layer was extracted by 0.8 mL phenol, followed by 0.6 mL chloroform. RNA was precipitated in 100% ethanol at 80°C for at least 24 h and reconstituted in nuclease-free water. Resuspended RNA was further purified using the RNeasy cleanup kit, and DNase digestion was carried out on the column (Qiagen, Inc.) according to the manufacturer's instructions.

Real-time reverse transcription–PCR. Purified RNA (1 μg) was reverse-transcribed by Superscript II enzyme (Invitrogen) and random hexamers. cDNA was cleaned-up using the Minelute PCR kit (Qiagen). cDNA (100-400 ng) was combined with TaqMan PCR Master Mix (Applied Biosystems) and run on an ABI PRISM 7000 Sequence Detection System using *Irx5* and 18S rRNA (endogenous control) specific primers and MGB probes (Applied Biosystems) as previously described (35). A standard curve was run to determine efficiency of primer/probe binding. All reactions were carried out in triplicate. RNA expression was quantified by the comparative δ-δ C_t method (Applied Biosystem's User Bulletin 2).

Cell proliferation. LNCaP cells (100,000 per well in six-well plates) were treated with indicated concentrations of $1,25(OH)_2D_3$ 24 h after plating. Cells were harvested by trypsinization 96 h after treatment and resuspended in media containing 0.4% trypan blue (Invitrogen). Live cells were counted under a microscope using a hemocytometer (Hausser Scientific).

Small interference RNA. Small interference (siRNA) molecules aligned with *Irx5* mRNA were synthesized by Dharmacon as desalted duplexes with the following sense sequences: si1 5′-GCC UCA GCG ACU CGG AUU UdT dT-3′, si2 5′-GAG AGA GAC AGA GAG AGA AdT dT-3′, si3 5′-CAU CGU CGG ACA AGG UCA AdT dT-3′. Cells were plated in RPMI 1640 containing 10% fetal bovine serum and transfected 36 h later with 133 μmol/L siRNA using Oligofectamine reagent (Invitrogen) in serum-free media according to the manufacturer's protocol. 10% Fetal bovine serum was added to transfected cells 4 h after transfection. Effects of *Irx5* knockdown were normalized to CY3-labeled luciferase GL2 duplex (control; Dharmacon) with target sequence 5′-CGT ACG CGG AAT ACT TCG A-3′.

Western blot analysis. LNCaP cells were washed twice in PBS and lysed in radioimmunoprecipitation assay buffer (1×PBS, 1% Nonidet P-40, 0.5% sodium deoxycholate, 0.1% SDS, 0.01% phenylmethylsulfonyl fluoride, 1× complete protease inhibitor cocktail; Roche). The lysate was incubated on ice for 1 h. Growth media containing dead cells was aspired and centrifuged for 5 min in chilled tabletop centrifuge at $4,000 \times g$. Pelleted cells were washed with PBS and combined with radioimmunoprecipitation assay buffer lysate. Cellular debris was pelleted in chilled microcentrifuge at $10,000 \times g$ for 30 min, and the supernatant was isolated. Protein concentrations were measured using Bradford reagent (Bio-Rad). Protein samples were resolved on a 10% NuPAGE precast gel (Invitrogen), transferred to a polyvinylidene difluoride membrane (Amersham), and probed with polyclonal antibody anti–poly (ADP-ribose) polymerase (PARP) p85 fragment (Promega) or polyclonal anti-p21 antibody (Santa Cruz). Loading control was accessed using monoclonal anti–β-tubulin antibody (Sigma), polyclonal anti-actin antibody, or anti–glyceraldehyde-3-phosphate dehydrogenase (Santa Cruz). A horseradish peroxidase–conjugated secondary antibody (Santa Cruz) was used to visualize proteins with standard luminol reagents (Perkin-Elmer Life Sciences, Inc.).

Hoechst staining. Trypsinized and floating cells were washed in PBS, pelleted, and resuspended in 3% paraformaldehyde/PBS solution (Sigma). To visualize apoptotic cells, cells were subsequently stained with Hoechst 33258 pentahydrate (Molecular Probes) and counted under a microscope with UV light source (excitation, 350-365 nmol/L). An average of 300 to 500 cells was counted per sample. Apoptotic cells with at least three nuclear fragments were scored and represented as a total of counted cells.

Overexpression. 1×10^5 per well LNCaP cells were plated into six-well plates. At ~60% confluency (36 h), cells were transfected with either 1 μg of the pCMV6/XL-5 (Origene) parent vector or the same vector containing the entire *Irx5* open reading frame using Lipofectamine (Invitrogen) according to the manufacturer's instructions.

Cell cycle analysis. Approximately 2×10^6 LNCap cells were harvested 48 and 72 h after treatment. Cells were washed in PBS, fixed in 70% ethanol for 1 h at 4°C, and stored for up to 2 wk at -20°C. At that time, cells were washed in PBS, stained with 1 mL of propidium iodide staining solution [3.8 mmol/L sodium citrate (Fisher Scientific) and 50 μg/mL propidium iodide (Sigma) in PBS], then combined with RNase A (Worthington Biochemicals), and added to a final

concentration of 0.5 μg/mL. Samples were stored at 4°C overnight and analyzed by flow cytometry on a FACSCalibur (Becton Dickson).

Statistical analysis. Means were compared using Student's *t* test or ANOVA when more than two samples were analyzed simultaneously.

Results

1,25(OH)$_2$D$_3$ down-regulates* Irx5 *in human prostate cancer tissue and in the androgen-sensitive prostate cancer cell line LNCaP. To explore the effects of 1,25(OH)$_2$D$_3$ on human prostate cancer, a randomized, placebo-controlled trial of high-dose 1,25(OH)$_2$D$_3$ before prostatectomy was carried out in patients with localized prostate cancer (34). After RNA extraction, the Affymetrix U133A chip was used to compare gene expression profiles in 10 prostate cancer specimens (samples confirmed to consist predominantly of adenocarcinoma by frozen section examined by a pathologist) collected after 4 weeks of high-dose 1,25(OH)$_2$D$_3$ or placebo therapy. The results showed that the homeobox gene *Irx5* is down-regulated in 1,25(OH)$_2$D$_3$-treated tumors relative to controls (raw P = 0.0000008, FDR = 33%; data not shown). Subsequently, the effect of 1,25(OH)$_2$D$_3$ therapy on down-regulation of *Irx5* expression was confirmed in the same human specimens using real-time reverse transcription–PCR (RT-PCR). As shown in Fig. 1A, *Irx5* mRNA levels, measured by real-time RT-PCR, are reduced 3-fold in 1,25(OH)$_2$D$_3$-treated patients compared with placebo-treated controls.

To further validate this target and develop a model system for laboratory investigation, the effect of 1,25(OH)$_2$D$_3$ (10^{-8} mol/L) on *Irx5* expression was examined in the LNCaP prostate cell line using real-time RT-PCR. A persistent 60% to 70% ($P < 0.001$, ANOVA) reduction in *Irx5* expression from 48 to 120 hours was observed with a single treatment of 1,25(OH)$_2$D$_3$ (10^{-8} mol/L; Fig. 1B). The presence of *Irx5* mRNA was also examined in androgen-independent PC-3 cancer cells and was found to be significantly lower in these cells (~30-fold lower than in LNCaP cells), as measured by real-time RT-PCR (data not shown).

Similar to the effects on LNCaP cells, *Irx5* mRNA expression is significantly down-regulated by 1,25(OH)$_2$D$_3$ in the hormone-dependent breast cancer cell line, MCF-7 (Fig. 1C). This experiment provides evidence that the effect of 1,25(OH)$_2$D$_3$

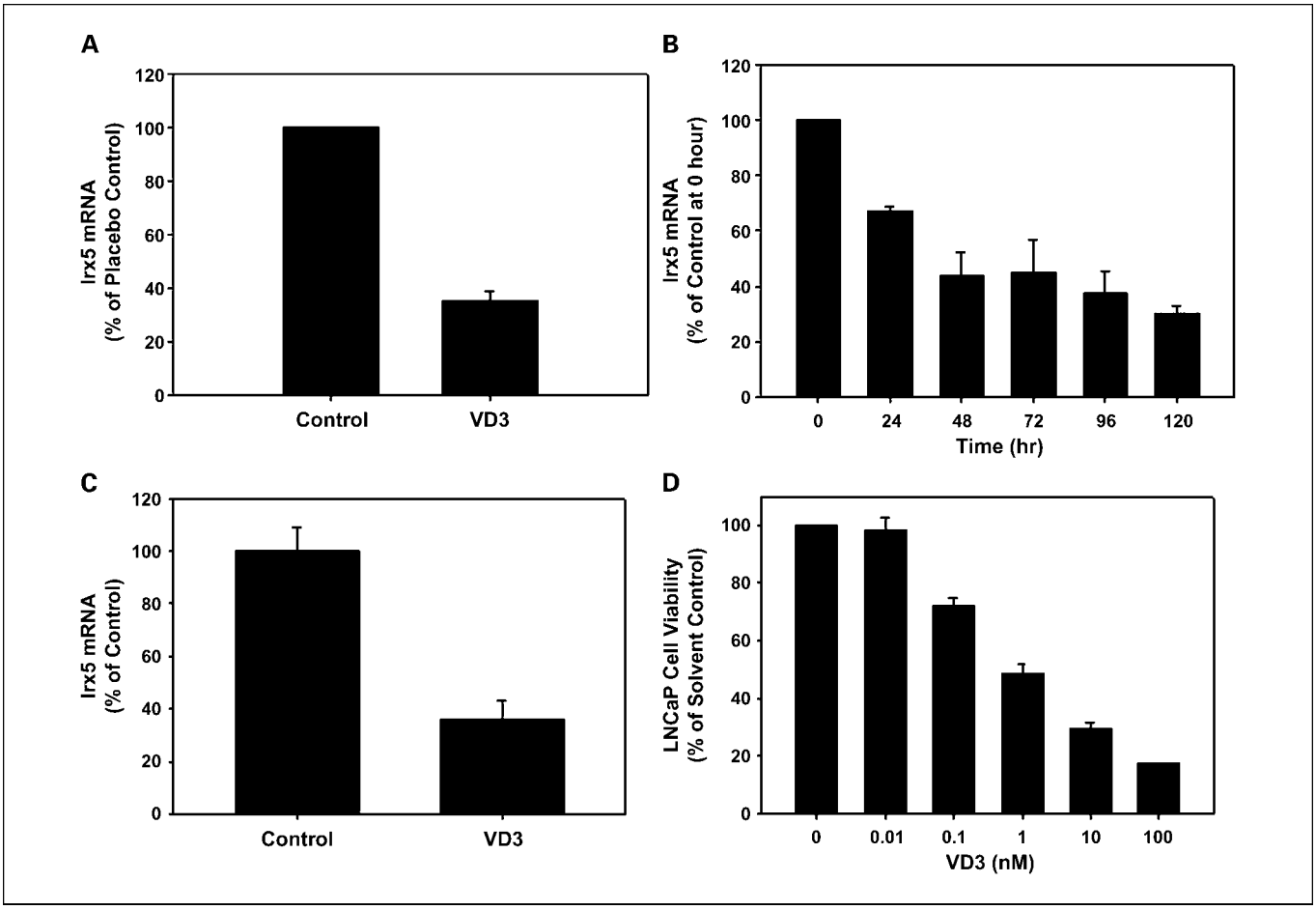

Fig. 1. 1,25(OH)$_2$D$_3$ (*VD3*) down-regulates expression of *Irx5* in human prostate cancer tissue (*A*), LNCaP cells (*B*), and MCF-7 cells (*C*). *A,* RNA was extracted from human prostate cancer tissue collected from patients treated weekly with either 0.5 μg/kg 1,25(OH)$_2$D$_3$ or placebo control for 4 wk before prostatectomy. mRNA of Irx5 was measured by real-time RT-PCR. Columns, mean of the placebo control; bars, SD. The difference is statistically significant ($P < 0.01$, *t* test). *B,* LNCaP cells treated with 1,25(OH)$_2$D$_3$ (10^{-8} mol/L) for 0 to 120 h. Levels of *Irx5* transcript were measured by real-time RT-PCR and normalized to 18S expression. At each time point, the difference is statistically significant ($P < 0.001$, ANOVA). *C,* Irx5 mRNA expression by real-time RT-PCR from MCF-7 cells treated with 1,25(OH)$_2$D$_3$ (10 nmol/L) for 96 h. The difference is statistically significant ($P < 0.005$, *t* test). *D,* dose-response effects of 1,25(OH)$_2$D$_3$ on LNCaP cell number. Cells were harvested 96 h after vitamin D treatment (0-100 nmol/L) and counted by a hemocytometer. Results are expressed as a mean percentage of control plates treated with ethanol vehicle. The differences are statistically significant starting with 0.1 nmol/L ($P < 0.01$) to 100 nmol/L ($P < 0.001$), *t* tests. Columns, means of three independent experiments; bars, SD.

on *Irx5* is not restricted to prostate cancer and may play a central role in other hormonally regulated tumors. $1,25(OH)_2D_3$ and its analogues have been shown to have significant antiproliferative effects on prostate cancer cells. The effect of $1,25(OH)_2D_3$ on LNCaP cell growth was examined over a range of concentrations to compare the effects of $1,25(OH)_2D_3$ with those resulting from targeting *Irx5* directly. A $1,25(OH)_2D_3$ dose-response curve shows that 10 nmol/L $1,25(OH)_2D_3$ reduces LNCaP cell numbers by ~50% at 96 hours ($IC_{50} \cong 10$ nmol/L; Fig. 1D).

Down-regulation of* Irx5 *by RNA interference reduces LNCaP cell numbers. To examine more closely the function of *Irx5* in prostate cancer cells, LNCaP cells were transfected with two different 21-nucleotide *Irx5*-specific siRNAs (si1 and si2) or control siRNA to knockdown *Irx5* expression, and viable cells were counted at 96 hours. *Irx5* si1 targets the open reading frame of the *Irx5* gene, and si2 targets the 3′ untranslated region. Transient transfection of siRNA oligos in LNCaP cells consistently exhibited ~60% transfection efficiency (data not shown). Treatment with si2 reduced *Irx5* gene expression by ~3-fold at 24 hours as determined by real-time RT-PCR (data not shown) and, as shown in Fig. 2A, was associated with a 50% reduction in LNCaP cell numbers ($P < 0.001$, *t* test) at 96 hours. A time course of the effect of si2 on LNCaP cell survival shows that cell numbers were reduced by ~60% at 120 hours compared with control siRNA-transfected cells (Fig. 2B).

All siRNA oligonucleotides were searched against the human genome, and no identical sequences were found. However, considering the possibility that *Irx5* RNA interference oligonucleotides may interact with a similar mRNA sequence in another gene, a third *Irx5* siRNA (si3) targeting the open reading frame of *Irx5* was tested to ensure that the effects observed were specific to *Irx5*. Figure 2C shows that this siRNA construct (si3) also significantly reduced LNCaP cell numbers at 96 hours compared with controls. When compared with the results with $1,25(OH)_2D_3$, *Irx5* knockdown had a similar effect on LNCaP cell survival at 96 hours as 10 nmol/L $1,25(OH)_2D_3$ (Fig. 1D). These data suggest that *Irx5* may serve as an important mediator for $1,25(OH)_2D_3$ sensitivity in LNCaP cells. Because specific *Irx5* down-regulation was found to have substantial inhibitory effects on prostate cancer cells, *Irx5* may function as a tumor promoter in these cells. In addition, MCF-7 breast (Fig. 3A) and HCT 116 colon cancer cells (Fig. 3B) transfected with *Irx5* siRNA (si2) showed significantly reduced cell numbers at 96 hours compared with transfection with a siRNA control, indicating that *Irx5* expression may be important in the regulation of a number of different tumor cells.

Down-regulation of* Irx5 *by RNA interference induces apoptosis of LNCaP cells. To examine the cellular mechanism of cell number reduction by *Irx5* knockdown, we determined if apoptosis is induced by *Irx5* gene targeting. Log-phase cultures were treated with siRNA *Irx5* (si2) or siRNA control and assessed for apoptosis by fluorescent microscopy. Figure 4A shows the difference in morphology between nonapoptotic control cells and apoptotic *Irx5* siRNA-transfected cells displaying several apoptotic bodies. *Irx5* knockdown resulted in apoptosis of ~15% of the cells at 120 hours compared with controls (Fig. 4B). The induction of apoptosis by *Irx5* siRNA was also shown by detection of the PARP cleavage product, a well-known marker of apoptosis (Fig. 4C; ref. 36). These data indicate that *Irx5* may use apoptosis as a primary means of regulating cell survival.

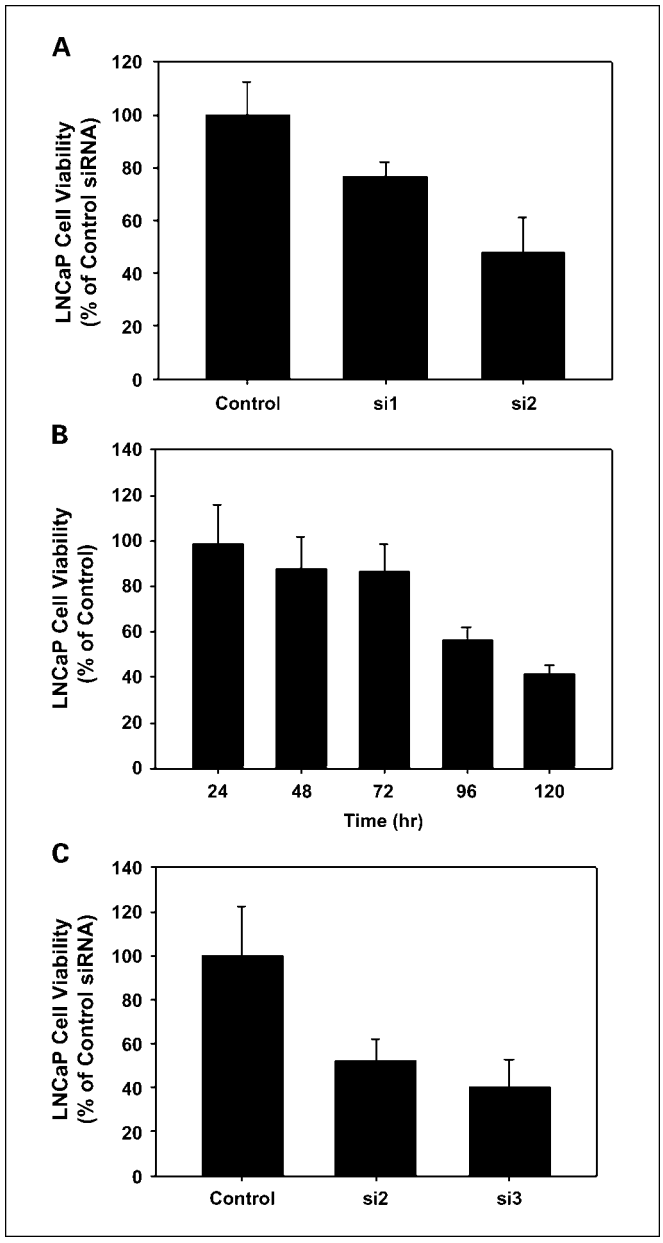

Fig. 2. Knockdown of *Irx5* by siRNA results in a reduction of LNCaP cell survival. LNCaP cells were transfected with either control (GL2) siRNA or *Irx5*-specific siRNA (si1, si2, or si3), and cells were counted using a hemocytometer. *A,* LNCaP cells were counted at 96 h after transfection with *Irx5* si1, si2, or control siRNA. Inhibition was statistically significant for si2 ($P < 0.001$ for si2, *t* test). *B,* LNCaP cell numbers at indicated time points after transfection with *Irx5* si2 or control siRNA. The difference between control and si2 is statistically significant ($P < 0.0002$, *t* test) at 96 and 120 h. *C,* LNCaP cell viability 96 h after transfection with *Irx5* si2, si3, or control siRNA. The difference between both si2 and si3 and control is statistically significant ($P < 0.00001$, *t* test). Results are expressed as mean percentage of control siRNA-transfected cells. Columns, mean of three independent experiments; bars, SD.

Decreased cell viability induced by* Irx5 *down-regulation is partially dependent upon p53 gene expression. Currently a role of *Irx5* or other *Irx* family members in signaling apoptosis has not been elucidated, and little is known about the mechanisms

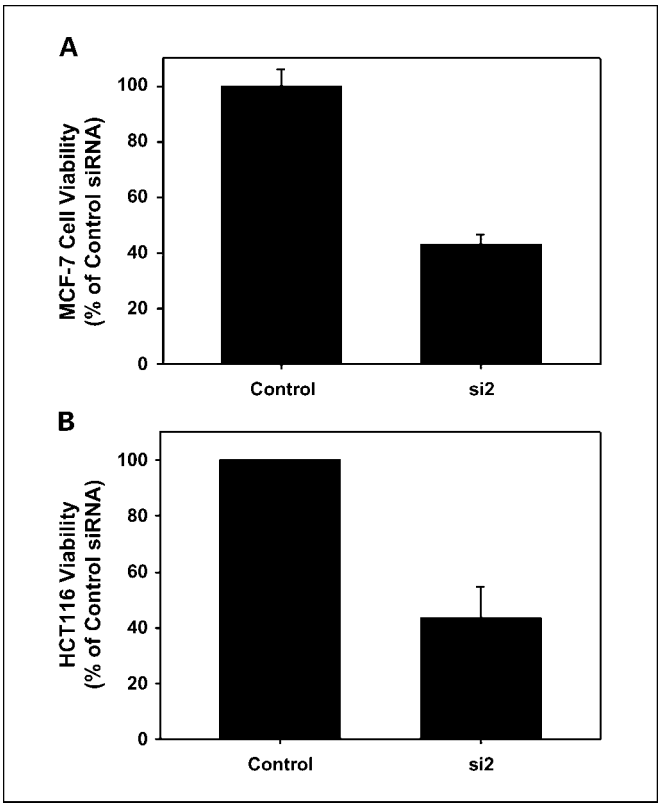

Fig. 3. Down-regulation of *Irx5* by siRNA results in decreased MCF-7 and HCT 116 cell number. MCF-7 (*A*) and HCT 116 (*B*) cells were counted 96 h after transfection with *Irx5* si2 or control siRNA. The differences between siRNA and control-treated cells are statistically significant in both experiments ($P < 0.0001$, *t* test). Results are expressed as mean percentage of control siRNA-transfected cells. Columns, mean of three independent experiments; bars, SD.

of apoptotic signaling by other homeobox genes. To study the effect of p53 on *Irx5*-mediated cell death, we used LNCaP cells that stably overexpress a dominant-negative p53 isoform (LNCaP-248, p53 DN). When *Irx5* was inhibited by siRNA interference in cells expressing mutant p53 proteins, PARP cleavage was decreased and delayed compared with LNCaP cells with empty vector controls (LNCaP-EV) that only have endogenous wild-type p53, indicating that the mechanism by which *Irx5* knockdown signals cell death is partially p53 dependent (Fig. 5A). Also, the usual reduction in cell numbers induced by *Irx5* down-regulation is partially abrogated in cells expressing mutant p53 proteins compared with LNCaP cells expressing p53 wild-type proteins (Fig. 5B; $P < 0.05$, *t* test). Furthermore, the wild-type endogenous p53 protein expression is increased (especially at 24 hours posttransfection) as a result of *Irx5* knockdown by siRNA (Fig. 5C), further supporting the involvement of p53 in the *Irx5* signaling pathway. Finally, when both LNCaP-EV and LNCaP-248 were treated with Tricostatin A, an HDAC inhibitor that induces p53-independent growth inhibition, similar inhibitory effects were observed in both cell lines (Fig. 5D).

Irx5 ***down-regulation induces more robust apoptosis than treatment with 10 nmol/L 1,25(OH)$_2$D$_3$.*** As shown above, the growth inhibitory effect of 10 nmol/L 1,25(OH)$_2$D$_3$ on LNCaP cell numbers is similar to that of *Irx5* down-regulation at 96 hours. To evaluate the degree of apoptosis induced by *Irx5* knockdown and that induced by 1,25(OH)$_2$D$_3$,we first compared the PARP cleavage induced by si3 and 10 nmol/L of 1,25(OH)$_2$D$_3$ (Fig. 6A). The result suggests that targeting *Irx5* directly may be a more effective strategy to induce apoptosis than treatment with 1,25(OH)$_2$D$_3$ (Fig. 6A). DNA staining (Hoechst) of 1,25(OH)$_2$D$_3$-treated cells (10 or 100 nmol/L) also suggests that 1,25(OH)$_2$D$_3$ is less efficient at inducing apoptosis than *Irx5* down-regulation (Fig. 6B). Targeting *Irx5* directly may be a more specific way to induce apoptosis and may prevent possible cross-talk from the induction of multiple pathways by vitamin D.

Irx5 ***down-regulation increases p21 protein expression and induces G$_2$-M arrest in LNCaP cells.*** In view of the well-described effects of vitamin D receptor ligands on cell cycle progression, we sought to examine the effect of Irx5 down-regulation on cell cycle progression and p21 expression. In

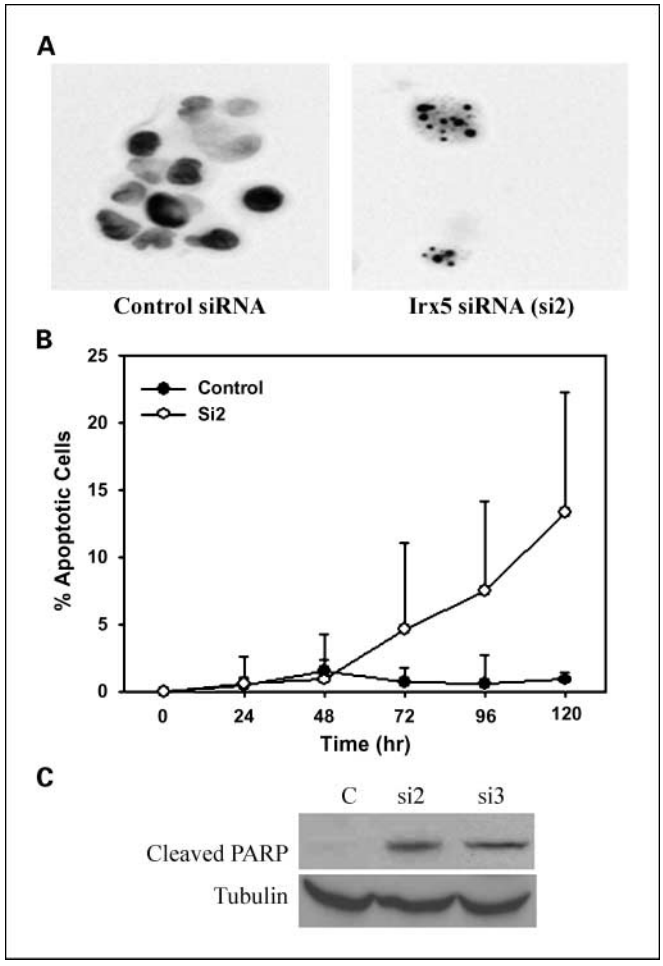

Fig. 4. Down-regulation of *Irx5* by siRNA induces apoptosis. Log-phase LNCaP cultures were transfected with *Irx5* (si2) or control siRNA at the indicated time points and stained with bis-benzimide (Hoechst). *A,* the difference in nuclear morphology between nonapopoptic (*left*) and apoptotic (*right*) cells was assessed by fluorescent microscopy in control and *Irx5* siRNA-treated cells. *B, Irx5* and control siRNA-transfected cells were harvested at the indicated time points and stained with bis-benzimide. The difference is statistically significant at 72, 96 ($P < 0.02$), and 120 h ($P = 0.001$, *t* test). Cells with at least three nuclear fragments were scored as apoptotic. Points, mean of triplicate experiments; bars, SD. *C,* knockdown of *Irx5* induces PARP cleavage. LNCaP cells were transfected with *Irx5* (si2 or si3) or control siRNA as indicated, and induction of apoptosis was shown by detection of the PARP p85 cleavage product by Western blots.

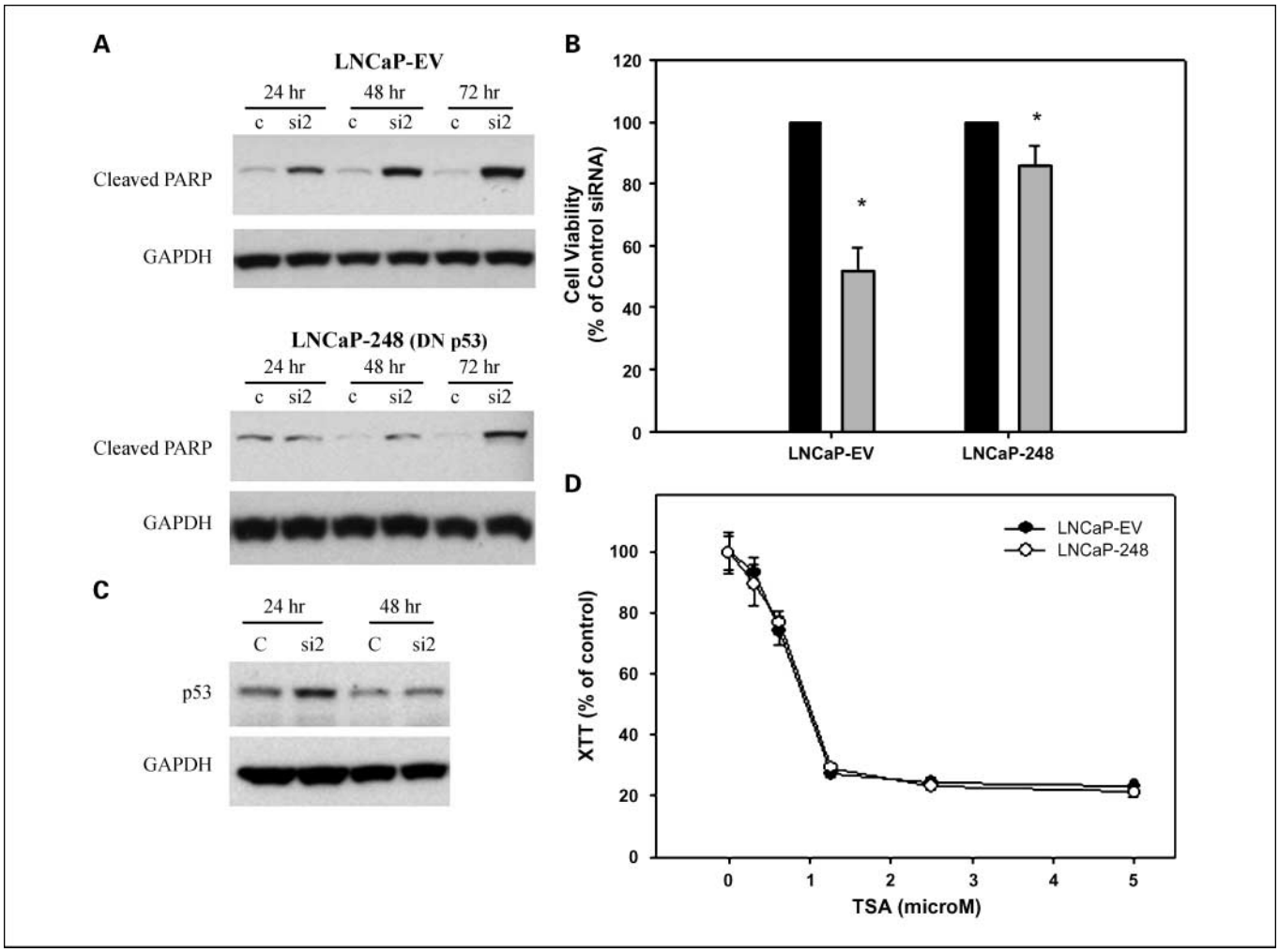

Fig. 5. Decreased cell viability induced by *Irx5* down-regulation is partially dependent upon p53 gene expression, and PARP cleavage is delayed and reduced in LNCaP cells stably expressing a p53 dominant-negative. *A,* LNCaP pC53Trp248 cells (LNCaP-248 mutant), expressing a dominant-negative p53 protein, and the control pRC-CMV (LNCaP-EV) cells were transfected with *Irx5* si2 or control siRNA. Proteins were harvested at the indicated time points, and anti-p85 PARP Western blots were carried out with a glyceraldehyde-3-phosphate dehydrogenase loading control. *B,* LNCaP-248 and control LNCaP-EV cells were transfected with *Irx5* si2 or control siRNA, and cells were counted 96 h later (*, $P < 0.01$, *t* test). *C,* protein extracts from LNCaP-EV cells transfected with Irx5 si2 or control siRNA were probed with anti-p53 antibody. All experiments were carried out in triplicate, and representative Western blots are shown. *D,* LNCaP-EV and LNCaP-248 cells exposed to 0.31, 0.62, 1.25, 2.5, or 5 μmol/L Tricostatin A for 48 h. Cell viability assessed using a standard 2,3-bis[2-methoxy-4-nitro-5-sulfophenyl]-2H-tetrazolium-5-carboxanilide inner salt (*XTT*) assay.

addition to apoptosis, down-regulation of *Irx5* by siRNA caused an increase in the cyclin-dependent kinase inhibitor p21 protein levels, indicating that *Irx5* may also regulate cell cycle progression (Fig. 7A). Interestingly, $1,25(OH)_2D_3$ has been shown to increase p21 protein expression in LNCaP cells. The observed increase in p21 protein levels was not preceded by an increase in p21 mRNA as measured by real-time RT-PCR (data not shown), suggesting that *Irx5* may be involved in regulating p21 protein stability rather than gene expression. To examine more directly the effects of *Irx5* on cell cycle regulation, we analyzed the cells by flow cytometry after their transfection with *Irx5* si2 or control siRNA. Figure 7B is a representation of the flow data in triplicate. *Irx5* knockdown resulted in a significant accumulation of cells in G_2-M, both at 48 and 72 hours, confirming that *Irx5* knockdown does indeed affect cell cycle progression and indicating that this may be through the regulation of p21 expression. Interestingly, the increase in p21 protein expression observed after *Irx5* knockdown is not affected by the absence of functional p53 protein (Fig. 7C) and therefore is not p53 dependent.

Overexpression of* Irx5 *decreases p21 and p53. To determine the effects of *Irx5* overexpression, LNCaP cells were transiently transfected with an *Irx5* overexpression vector containing the *Irx5* open reading frame or empty vector control. *Irx5* overexpression reduced both p21 and p53 protein levels at the indicated time points in LNCaP cells (Fig. 8A and B). This provides further evidence of a role of *Irx5* in cell cycle regulation.

Discussion

To our knowledge, this is the first report to show that *Irx* genes are involved in the regulation of apoptosis and cell cycle arrest in human prostate cancer cells. However, recently, it has been shown that an antisense oligodeoxynucleotide capable of simultaneously inducing the loss of *Irx1-3* and *Irx5* expression

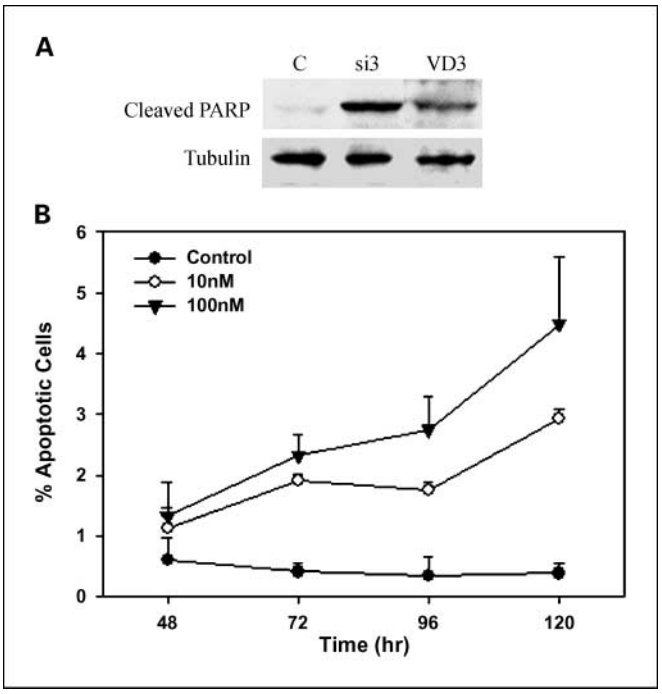

Fig. 6. $1,25(OH)_2D_3$ induces apoptosis in LNCaP cells. *A,* LNCaP extracts treated with 10 nmol/L $1,25(OH)_2D_3$ or *Irx5* si3 or control siRNA (*C*) were probed for cleaved PARP. *B,* LNCaP cells treated with either 10 or 100 nmol/L $1,25(OH)_2D_3$ were harvested at the indicated time points and stained with bis-benzimide. Cells with at least three nuclear fragments were scored as apoptotic. The differences between $1,25(OH)_2D_3$ and control are significantly different at all time points ($P < 0.0015$ for 10 nmol/L at 24 h, $P < 0.0001$ at all other time points and concentrations, *t* tests). Experiments were carried out in triplicate. Points, mean of triplicate experiments; bars, SD.

in developing lung explants dramatically increased apoptosis of the mesenchymal cells while decreasing cell proliferation (37).

Knockdown of *Irx5* leads to an increase in p53 protein expression. We were not able to detect specific phosphorylated/activated species of p53 in our parental LNCaP protein extracts but did observe phosphorylation of two specific serines in our LNCaP 248 cells, which express high levels of mutant p53 proteins. In the p53 mutant cells, phosphorylation of Ser^{15}, which is thought to be involved in p53 ubiquitination/degradation, was increased by *Irx5* knockdown, whereas phosphorylation of Ser^{392}, which is involved in p53-induced transcriptional activation, was increased after transfection with *Irx5* si2 (data not shown). LNCaP cells expressing mutant p53 proteins also were partially resistant to the growth inhibitory effects of *Irx5* knockdown, and PARP cleavage in these cells was delayed and reduced compared with p53 wild-type controls. However, PARP cleavage was increased in the p53 mutant cells after *Irx5* knockdown, indicating that at least in part PARP cleavage is p53 independent.

p21 protein expression in both p53 wild-type and dominant-negative mutant cells was similarly increased by the knockdown of *Irx5*, suggesting that the effect of *Irx5* on p21 is p53 independent as well. Multiple studies have shown that p21 is induced by both p53-dependent and p53-independent mechanisms. A number of transcription factors, including Sp1, Sp3, MyoD, STAT proteins, and CAAT/enhancer binding proteins activate p21 transcription via p53-independent pathways (38), and recently, it has been suggested that p21, in addition to inhibiting the cell cycle, also plays a role in regulating cell death (39). Most of this evidence indicates that p21 protects cells against apoptosis, but a number of reports have shown p21 to be proapoptotic in certain models, and studies in p21-deficient mice suggest that p21 is involved in tumor suppression (40). We found that p21 protein expression is up-regulated by *Irx5* knockdown while p21 mRNA remains unchanged, suggesting the regulation of p21 by posttranscriptional modifications or reduced ubiquitination. p21 expression has previously been

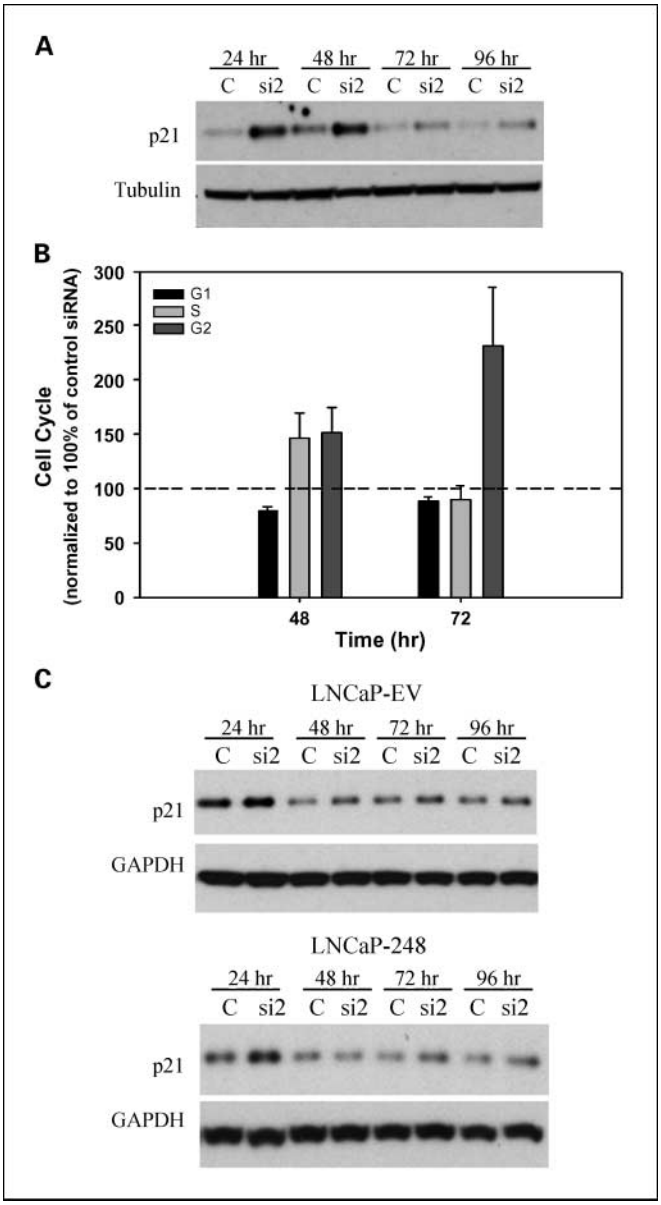

Fig. 7. p21 protein expression is increased by *Irx5* down-regulation. *A,* LNCaP cells were transfected with *Irx5* si2 or control siRNA (*C*) and proteins were harvested at the indicated time points. An anti-p21 antibody was used to probe protein blots. This experiment was carried out multiple times, and a representative Western blot is shown. *B,* results of flow cytometry at 48 and 72 h, showing the percentage of cells in G_1, S, and G_2-M as normalized to control siRNA transfected cells. *C,* increased p21 protein expression after *Irx5* knockdown is not affected by the absence of functional p53 protein. Protein extracts from LNCaP pC53Trp248 (LNCaP-248) and control pRC-CMV LNCaP (LNCaP-EV) cells transfected with *Irx5* si2 or control siRNA were probed with anti-p21 antibody. All experiments were carried out in triplicate, and representative Western blots are shown. Columns, mean of three independent experiments; bars, SD.

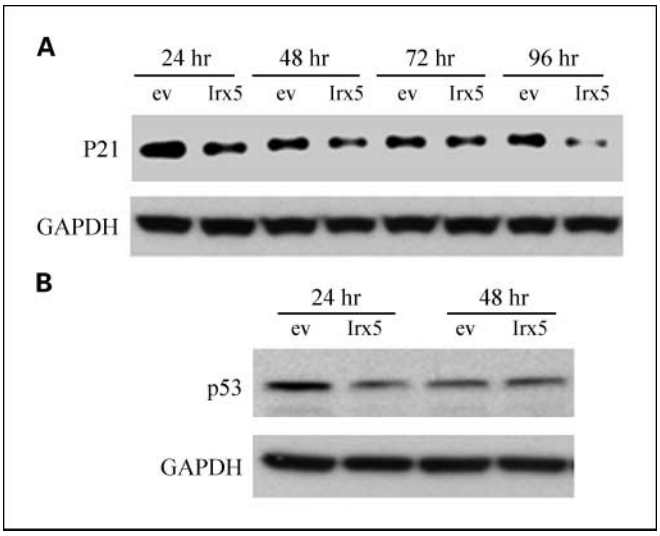

Fig. 8. Overexpression of *Irx5* decreases p21 and p53 protein expression. *A,* LNCaP cells transiently transfected with an *Irx5* overexpression vector have reduced p21 expression at the indicated time points by Western blot analysis. *B,* LNCaP cells transfected with the Irx5 overexpression vector also have reduced p53 protein expression at 24 h. All experiments were carried out in triplicate, and representative Western blots are shown.

found to be regulated by both ubiquitin-dependent and ubiquitin-independent degradation (41–43).

Although the cyclin-dependent kinase inhibitor p21 has recently been shown to be involved in the regulation of apoptosis, cell senescence, transcription of several genes, and genome stability (44), p21 is best known for its role in inhibiting the cell cycle. p21 causes cell cycle arrest mainly by inhibiting several of the cyclin/cyclin-dependent kinase complexes, which in turn regulate progression through the cell cycle by reducing phosphorylation of the Rb protein/inactivating members of the retinoblastoma family (38). Depending on the cell type and experimental conditions, ectopic expression of p21 leads to G_1-phase, G_2-phase, or S-phase arrest (45, 46). We have shown here that an increase in p21 protein expression induced by a reduction in *Irx5* accompanies the G_2-M cell cycle arrest, indicating that p21 may be responsible for this arrest.

Irx5 has not previously been linked to the effects of vitamin D, but in primary cultures of embryonic quail cardiomyocytes, a complex composed of the *Irx4* protein, vitamin D receptor and retinoic X receptor α binds the vitamin D response element in the slow myosin heavy chain 3 gene to repress transcription. The slow MyHC3 gene is one of the earliest atrial chamber-specific genes expressed during cardiogenesis (23). This suggests that Iroquois proteins may play a role in vitamin D receptor signaling.

Misexpression of many homeobox genes has been detected in a number of cancers. An elegant study by Gidekel et al. showed that the aberrant expression of the homeobox gene Oct-4 increases the tumorigenic potential of embryonic stem cells and is required for maintenance of the malignant phenotype (47). Homeobox genes also seem to be involved in cell differentiation. *Xiro1* (an *Iro* gene identified in *Xenopus*) represses the orthologue of mammalian *Gadd45*γ, which antagonizes neuronal differentiation in *Xenopus* early development (48). Recently, *Irx5* expression was identified in postnatal bipolar interneurons during retinal development and may play a role in the differentiation of these cells (49). Homeobox genes also seem to play a role in regulating apoptosis, angiogenesis, and metastasis; however, very little is known about the specific signaling pathways involved (31, 32). In numerous embryonic tissue types, Iroquois gene expression is regulated spatially and temporally by a number of different signaling pathways, including Sonic Hedgehog, Wingless, Notch, epidermal growth factor receptor, and Hox signaling. Interestingly, these pathways have all been implicated in tumorigenesis.

In the present study, we have shown that the homeobox protein *Irx5* is down-regulated by $1,25(OH)_2D_3$ in human prostate cancer tissue, in the prostate cancer cell line LNCaP, and in MCF-7 breast cancer cells. *Irx5* knockdown in LNCaP cells leads to a reduction in cell number, increased p21 and p53 protein expression, G_2-M cell cycle arrest, and increased apoptosis and also results in reduced cell survival in the colon cancer cell line HCT 116 and in MCF-7 cells. Conversely, forced expression of *Irx5* increases p21 and p53 expression. These data indicate that *Irx5* may be a promising new therapeutic target in cancer treatment.

Disclosure of Potential Conflicts of Interest

No potential conflicts of interest were disclosed.

Acknowledgments

We thank Dr. Milan Uskokovic (Roche) for the generous supply of $1,25(OH)_2D_3$ for *in vitro* experiments, Oregon Health and Science University Affymetrix Microarray Core Facility and Mandy Boyd from Oregon Health and Science University Cancer Center Flow Cytometry Core Facility for invaluable assistance and advice, Jane Yates for RNA extraction from human tissue, and Motomi Mori for statistical analysis.

References

1. Guyton KZ, Kensler TW, Posner GH. Vitamin D, vitamin D. analogs as cancer chemopreventive agents. Nutr Rev 2003;61:227–38.
2. Johnson CS, Hershberger PA, Bernardi RJ, McGuire TF, Trump DL. Vitamin D receptor: a potential target for intervention. Urology 2002;60:123–30; discussion 30–1.
3. Guzey M, Kitada S, Reed JC. Apoptosis induction by 1α,25-dihydroxyvitamin D3 in prostate cancer. Mol Cancer Ther 2002;1:667–77.
4. Modzelewski RA, Hershberger PA, Johnson CS, Trump DL. Apoptotic effects of paclitaxel and calcitriol in rat dunning MLL and human PC-3 prostate tumors *in vitro*. Proc AACR 1999;40:580.
5. Pepper C, Thomas A, Hoy T, Milligan D, Bentley P, Fegan C. The vitamin D3 analog EB1089 induces apoptosis via a p53-independent mechanism involving p38 MAP kinase activation and suppression of ERK activity in B-cell chronic lymphocytic leukemia cells *in vitro*. Blood 2003;101:2454–60.
6. Bektas M, Orfanos CE, Geilen CC. Different vitamin D analogues induce sphingomyelin hydrolysis and apoptosis in the human keratinocyte cell line HaCaT. Cell Mol Biol (Noisy-le-grand) 2000;46:111–9.
7. Bernardi RJ, Trump DL, Yu WD, McGuire TF, Hershberger PA, Johnson CS. Combination of 1α,25-dihydroxyvitamin D(3) with dexamethasone enhances cell cycle arrest and apoptosis: role of nuclear receptor cross-talk and Erk/Akt signaling. Clin Cancer Res 2001;7:4164–73.
8. McGuire TF, Trump DL, Johnson CS. Vitamin D(3)-induced apoptosis of murine squamous cell carcinoma cells. Selective induction of caspase-dependent MEK cleavage and up-regulation of MEKK-1. J Biol Chem 2001;276:26365–73.
9. Bernardi R, Johnson CS, Modzelewski RA, Trump, DL. Antiproliferative effects of 1α,25-dihydroxyvitamin D3 and vitamin D analogs on tumor-derived endothelial cells. Endocrinology 2002;143:2508–14.
10. Mantell DJ, Owens PE, Bundred NJ, Mawer EB, Canfield AE. 1 α,25-dihydroxyvitamin D(3) inhibits

angiogenesis *in vitro* and *in vivo*. Circ Res 2000; 87:214–20.

11. Majewski S, Skopinska M, Marczak M, Szmurlo A, Bollag W, Jablonska S. Vitamin D3 is a potent inhibitor of tumor cell-induced angiogenesis. J Investig Dermatol Symp Proc 1996;1:97–101.

12. Getzenberg RH, Light BW, Lapco PE, et al. Vitamin D inhibition of prostate adenocarcinoma growth and metastasis in the Dunning rat prostate model system. Urology 1997;50:999–1006.

13. Schwartz GG, Wang MH, Zhang M, Singh RK, Siegal GP. 1α, 25-dihydroxyvitamin D (calcitriol) inhibits the invasiveness of human prostate cancer cells. Cancer Epidemiol Biomarkers Prev 1997;6: 727–32.

14. Sung V, Feldman D. 1,25-Dihydroxyvitamin D3 decreases human prostate cancer cell adhesion and migration. Mol Cell Endocrinol 2000;164:133–43.

15. Dambly-Chaudiere C, Leyns L. The determination of sense organs in *Drosophila*: a search for interacting genes. Int J Dev Biol 1992;36:85–91.

16. Leyns L, Gomez-Skarmeta JL, Dambly-Chaudiere C. iroquois: a prepattern gene that controls the formation of bristles on the thorax of *Drosophila*. Mech Dev 1996;59:63–72.

17. Bellefroid EJ, Kobbe A, Gruss P, Pieler T, Gurdon JB, Papalopulu N. Xiro3 encodes a *Xenopus* homolog of the *Drosophila* Iroquois genes and functions in neural specification. EMBO J 1998;17:191–203.

18. Bosse A, Stoykova A, Nieselt-Struwe K, et al. Identification of a novel mouse Iroquois homeobox gene, Irx5, and chromosomal localisation of all members of the mouse Iroquois gene family. Dev Dyn 2000;218: 160–74.

19. Gomez-Skarmeta JL, Glavic A, de la Calle-Mustienes E, Modolell J, Mayor R. Xiro, a *Xenopus* homolog of the *Drosophila* Iroquois complex genes, controls development at the neural plate. EMBO J 1998;17:181–90.

20. Goriely A, Diez del Corral R, Storey KG. c-Irx2 expression reveals an early subdivision of the neural plate in the chick embryo. Mech Dev 1999;87:203–6.

21. Peters T, Dildrop R, Ausmeier K, Ruther U. Organization of mouse Iroquois homeobox genes in two clusters suggests a conserved regulation and function in vertebrate development. Genome Res 2000;10: 1453–62.

22. Gomes-Skarmeta JL, Diez del Corral R, de la Calle-Mustiennes E, Ferres-Marco D, Modolell J. *araucan* and *caupolican*, two members of the novel Iroquois complex, encode homeoproteins that control proneural and vein-forming genes. Cell 1996;85:95–105.

23. Wang GF, Nikovits W, Jr., Bao ZZ, Stockdale FE. Irx4 forms an inhibitory complex with the vitamin D, retinoic X. receptors to regulate cardiac chamber-specific slow MyHC3 expression. J Biol Chem 2001;276: 28835–41.

24. Kudoh T, Dawid IB. Role of the iroquois3 homeobox gene in organizer formation. Proc Natl Acad Sci U S A 2001;98:7852–7.

25. Bilioni A, Craig G, Hill C, McNeill H. Iroquois transcription factors recognize a unique motif to mediate transcriptional repression *in vivo*. Proc Natl Acad Sci U S A 2005;102:14671–6.

26. Stuart ET, Yokota Y, Gruss P. PAX and HOX in neoplasia. Adv Genet 1995;33:255–74.

27. De Vita G, Barba P, Odartchenko N, et al. Expression of homeobox-containing genes in primary and metastatic colorectal cancer. Eur J Cancer 1993;29A: 887–93.

28. Friedmann Y, Daniel CA, Strickland P, Daniel CW. Hox genes in normal and neoplastic mouse mammary gland. Cancer Res 1994;54:5981–5.

29. Abate-Shen C. Deregulated homeobox gene expression in cancer: cause or consequence? Nat Rev Cancer 2002;2:777–85.

30. Del Bene F, Wittbrodt J. Cell cycle control by homeobox genes in development and disease. Semin Cell Dev Biol 2005;16:449–60.

31. Chen H, Sukumar S. Role of homeobox genes in normal mammary gland development and breast tumorigenesis. J Mammary Gland Biol Neoplasia 2003; 8:159–75.

32. Lohmann I, McGinnis N, Bodmer M, McGinnis W. The *Drosophila* Hox gene deformed sculpts head morphology via direct regulation of the apoptosis activator reaper. Cell 2002;110:457–66.

33. Daftary GS, Taylor HS. Endocrine regulation of HOX genes. Endocr Rev 2006;27:331–55.

34. Beer TM, Myrthue A, Garzotto M, et al. Randomized study of high-dose pulse calcitriol or placebo prior to radical prostatectomy. Cancer Epidemiol Biomarkers Prev 2004;13:2225–32.

35. Iwao K, Miyoshi Y, Egawa C, Ikeda N, Noguchi S. Quantitative analysis of estrogen receptor-β mRNA and its variants in human breast cancers. Int J Cancer 2000;88:733–6.

36. Duriez PJ, Shah GM. Cleavage of poly(ADP-ribose) polymerase: a sensitive parameter to study cell death. Biochem Cell Biol 1997;75:337–49.

37. van Tuyl M, Liu J, Groenman F, et al. Iroquois genes influence proximo-distal morphogenesis during rat lung development. Am J Physiol Lung Cell Mol Physiol 2006;290:L777–89.

38. Gartel AL, Tyner AL. Transcriptional regulation of the p21 ((WAF1/CIP1)) gene. Exp Cell Res 1999;246: 280–9.

39. Gartel AL, Tyner AL. The role of the cyclin-dependent kinase inhibitor p21 in apoptosis. Mol Cancer Ther 2002;1:639–49.

40. Martin-Caballero J, Flores JM, Garcia-Palencia P, Serrano M. Tumor susceptibility of p21(Waf1/Cip1)-deficient mice. Cancer Res 2001;61:6234–8.

41. Maki CG, Howley PM. Ubiquitination of p53 and p21 is differentially affected by ionizing and UV radiation. Mol Cell Biol 1997;17:355–63.

42. Sheaff RJ, Singer JD, Swanger J, Smitherman M, Roberts JM, Clurman BE. Proteasomal turnover of p21Cip1 does not require p21Cip1 ubiquitination. Mol Cell 2000;5:403–10.

43. Touitou R, Richardson J, Bose S, Nakanishi M, Rivett J, Allday MJ. A degradation signal located in the C-terminus of p21WAF1/CIP1 is a binding site for the C8 α-subunit of the 20S proteasome. EMBO J 2001;20:2367–75.

44. Roninson IB. Oncogenic functions of tumour suppressor p21 (Waf1/Cip1/Sdi1): association with cell senescence and tumour-promoting activities of stromal fibroblasts. Cancer Lett 2002;179:1–14.

45. Niculescu AB III, Chen X, Smeets M, Hengst L, Prives C, Reed SI. Effects of p21 (Cip1/Waf1) at both the G_1-S and the G_2-M cell cycle transitions: pRb is a critical determinant in blocking DNA replication and in preventing endoreduplication. Mol Cell Biol 1998;18: 629–43.

46. Ogryzko VV, Wong P, Howard BH. WAF1 retards S-phase progression primarily by inhibition of cyclin-dependent kinases. Mol Cell Biol 1997;17:4877–82.

47. Gidekel S, Pizov G, Bergman Y, Pikarsky E. Oct-3/4 is a dose-dependent oncogenic fate determinant. Cancer Cell 2003;4:361–70.

48. de la Calle-Mustienes E, Glavic A, Modolell J, Gomez-Skarmeta JL. Xiro homeoproteins coordinate cell cycle exit and primary neuron formation by upregulating neuronal-fate repressors and downregulating the cell-cycle inhibitor XGadd45-γ. Mech Dev 2002; 119:69–80.

49. Cheng CW, Chow RL, Lebel M, et al. The Iroquois homeobox gene, Irx5, is required for retinal cone bipolar cell development. Dev Biol 2005;287:48–60.